Final Performance Report – July 2023

RIEMANN SURFACES IN LAYERED VAN DER WAALS NANOWIRES: PRECISION TWIST MOIRÉS, NANOSCALE SOLENOIDS, AND SCREW DISLOCATION SPIN-ORBIT COUPLING

ONR Award No. N00014-20-1-2305

Office of Naval Research Program Office:
Nanoelectronics Program, ONR Code 31 Information, Cyber and Spectrum Superiority

ONR Technical Point of Contact:
Lennart (Dan) Gunlycke, D.Phil., lennart.d.gunlycke.civ@us.navy.mil
Chagaan Baatar, Ph.D., chagaan.baatar.civ@mail.mil

Principal Investigators:
Prof. Peter Sutter, Electrical & Computer Engineering, University of Nebraska-Lincoln
Prof. Eli Sutter, Mechanical & Materials Engineering, University of Nebraska-Lincoln

Table of Contents

1. Major Project Goals

Van der Waals (vdW) heterostructures of atomically thin (two-dimensional, 2D) crystals promise materials integration without the conventional lattice-matching constraints governing 3D-crystalline materials. Of particular interest are twisted stacks in which the constituent lattices are misaligned by a small azimuthal angle. Prior work has shown that interfacial moiré patterns in twisted homo- and heterostructures support emergent properties such as moiré excitons and phonons, as well as strongly correlated behavior of charge carriers due to ultra-narrow flat bands at small interlayer twist. To date, such twisted structures have been realized primarily in a planar geometry and fabricated by mechanical stacking, which is challenging, especially at small twist angles.

This research project built on the discovery by the PIs that nanowires of layered vdW crystals, synthesized by vapor-liquid-solid (VLS) growth, can provide a new architecture for realizing interlayer twists. VdW nanowires show a strong propensity toward incorporating axial screw dislocations, and Eshelby twist due to the dislocation stress field spontaneously produces a chiral structure. The resulting helical layered nanowires represent a scalable platform for realizing vdW interfaces with small twist angles that are controlled by the wire diameter and stabilized by the axial screw dislocation (Figure 1).

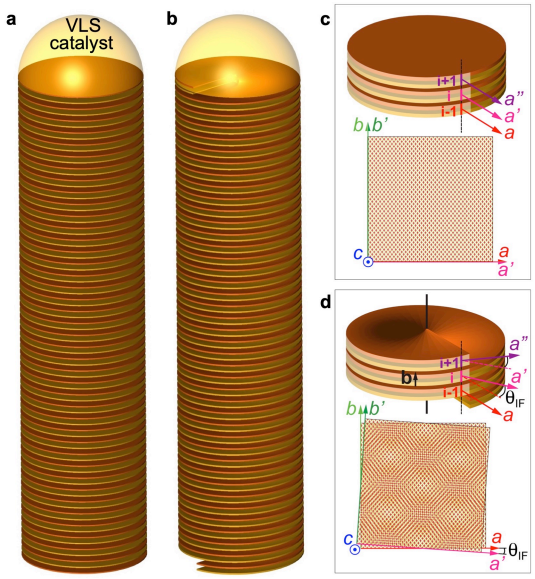

Figure 1. Chiral twisted van der Waals nanowires. a. Schematic rendering of a layered vdW nanowire. A molten metal VLS catalyst at the nanowire tip supplies material from the vapor phase to the growth front, thus mediating nucleation of new layers and 1D growth of a nanowire whose diameter is determined by the size of the catalyst. **b.** Schematic rendering of a chiral twisted vdW nanowire hosting an axial screw dislocation. The chiral nanowire grows without nucleation *via* spiral growth from material supplied by the molten metal VLS catalyst. **c.** Layering in an ordinary (defect-free) vdW nanowire. Adjacent layers form an aligned interface, analogous to a bulk crystal of the same material. **d.** Small-angle twist interfaces in chiral twisted vdW nanowires. Due to the helical structure caused by the axial screw dislocation, groups of layers separated by one Burgers vector (**b**) of the dislocation form a twisted interface (with twist angle θ_{IF}) harboring a twist moiré pattern. Governed by Eshelby twist, the interlayer twist angle (and hence the periodicity of the interlayer moiré) is defined by the diameter of the wire, where thinner wires have larger interlayer twist angles (smaller moiré periods).

A primary objective of the work under this project has been to explore how such precisely tunable interlayer twists affect optoelectronics, interlayer phonons, and charge transport in vdW nanowires. Realizing this goal required the successful completion of several interconnected tasks. First and foremost, VLS growth and related processes needed to be developed to *(i)* obtain nanowires with different diameters so as to realize different interlayer twists; *(ii)* extend the concept of twisted chiral vdW nanowires and related layered 1D nanostructures to new materials; and *(iii)* achieve novel architectures, such as homojunctions between twisted and ordinary layered segments in single nanowires, thereby creating structures that can support a deeper understanding of the functional properties caused by interlayer twist in vdW nanowires.

New approaches were developed to assess the emerging properties on individual nanowires. To access optoelectronics and photonics, the project benefited from far-reaching capabilities in the laboratories of the PIs for creating excited states at the nanometer scale using nanometer-focused high-energy electron beams in scanning transmission electron microscopy and probing radiative relaxation by cathodoluminescence spectroscopy (STEM-CL). Such nanoscale luminescence experiments were complemented by local optical absorption measurements using monochromated valence electron energy loss spectroscopy (EELS). Single-nanowire Raman spectroscopy and electrical measurements aimed to establish the effect of the twisted chiral structure on phonons and charge transport.

Beyond the physics of small-angle twist moirés in nanowires, the helical structure and axial screw dislocations offer additional opportunities for significant scientific advances. Another main objective of the project has been to establish the materials science required to realize these systems and to identify the physical principles governing their function. For example, chiral twisted vdW nanowires can provide a novel approach toward shrinking inductors and electromagnets – devices that have largely been bypassed by scaling in microelectronics – to nanometer dimensions if ways can be developed to force moving charges along the helical path within the layers rather than across the interlayer gaps. To this end, the project explored the synthesis of heterostructures in which a wide-bandgap vdW semiconductor core serves as a scaffold for the synthesis of a highly conducting helical shell.

Finally, the project has contributed to exploring other emerging phenomena in vdW nanostructures. Symmetry breaking by a chiral structure, for example, can open new avenues toward ferroelectricity. Screw dislocations in nanowires were theoretically predicted to cause novel spin-orbit coupling effects and produce spin textures with long coherence times. And there is growing awareness of unusual electronic and topological effects associated with lattice defects such as dislocations. The potential of dislocated vdW nanowires for ferroelectrics, spintronics, and emergent electronic phenomena may be explored by charge- and spin-transport experiments on suitable test device structures. Such research is part of the longer-term outlook beyond the lifetime of this project.

The technical approach combined established methods, such as materials synthesis by vapor transport and characterization by optical and electron microscopy, micro-Raman spectroscopy, *etc.*, with techniques at the very forefront of the field. In particular, optoelectronic properties were measured at the moiré length scale by combined electron-beam excited luminescence and absorption spectroscopies, locally correlated with structural probes on the same vdW nanowires.

With its successful completion, the project has provided a fundamental understanding of the effects of interlayer twist moirés on the electronic structure, optoelectronics, and photonics for a unique nanowire-based van der Waals architecture that allows the precise selection and

stabilization of small-angle interlayer twist. And it has paved the way for developing helical nanowires into scalable inductors and solenoids, as well as spin- and charge-transport channels. While clearly in the realm of fundamental research, the research contributes to technologies critical to the Navy and DOD, notably in optoelectronics and photonics relevant for classical and quantum information processing, and by raising the prospect of using chiral nanowires in novel device elements, *e.g.*, with the capability of locally generating high magnetic fields on demand. In addition to the scientific and potential technological benefits, the project has contributed to the education and training of the military and civilian high-technology workforce *via* training and mentoring of the participating students and postdocs.

2. Accomplishments

2.1. VLS growth and optoelectronics of GaS vdW nanowires [*ACS Nano 14, 6117 (2020)*]

In our prior work, chiral twisted vdW nanowires were obtained from GeS, an orthorhombic group IV chalcogenide. The fact that twist moiré effects (*e.g.*, Hubbard model correlated physics) were predicted and reported for hexagonal 2D crystals (graphene, TMDs) motivated extending the synthesis of twisted nanowires to systems with hexagonal symmetry.

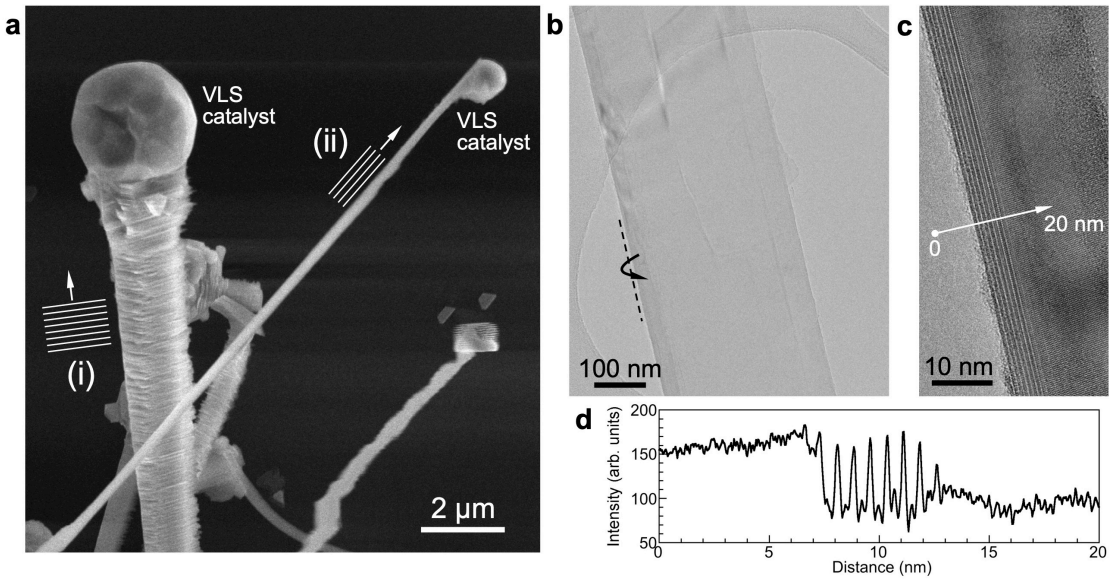

Figure 2. Layer orientation in VLS grown GaS nanowires. a. SEM image showing the two nanowire types obtained by VLS growth of GaS over Ag catalysts: *(i)* Tapered longitudinally layered wires (vdW layers perpendicular to the wire axis), and *(ii)* ribbon-like transverse layered wires (layers parallel to the wire axis). **b.** TEM image of an ultrathin GaS ribbon whose edge is folded to show the number of layers. **c.** High-resolution TEM image of the wire shown in b. **d.** Intensity profile across the edge (arrow in c.), showing a thickness of 8 GaS tetralayers.

We identified conditions for growing high-quality vdW nanowires of hexagonal GaS using two VLS catalysts: Au and Ag. While GeS crystallizes with uniform longitudinal layering (layers perpendicular to nanowire axis), GaS showed a complex behavior (Figure 2). Au catalysts consistently yield transverse layered ribbon-like nanowires (layers parallel to wire axis). Ag catalysts produce both longitudinal and transverse layered wires, *i.e.*, both of the canonical layering directions in nanowires. Mirror-twins (rather than screw dislocations) were the prevalent

defects in longitudinal wires, and GaS has not yet yielded twisted nanowires. However, our results provided insight into the VLS synthesis of Ga chalcogenide nanowires, as well as their optoelectronics and photonics.

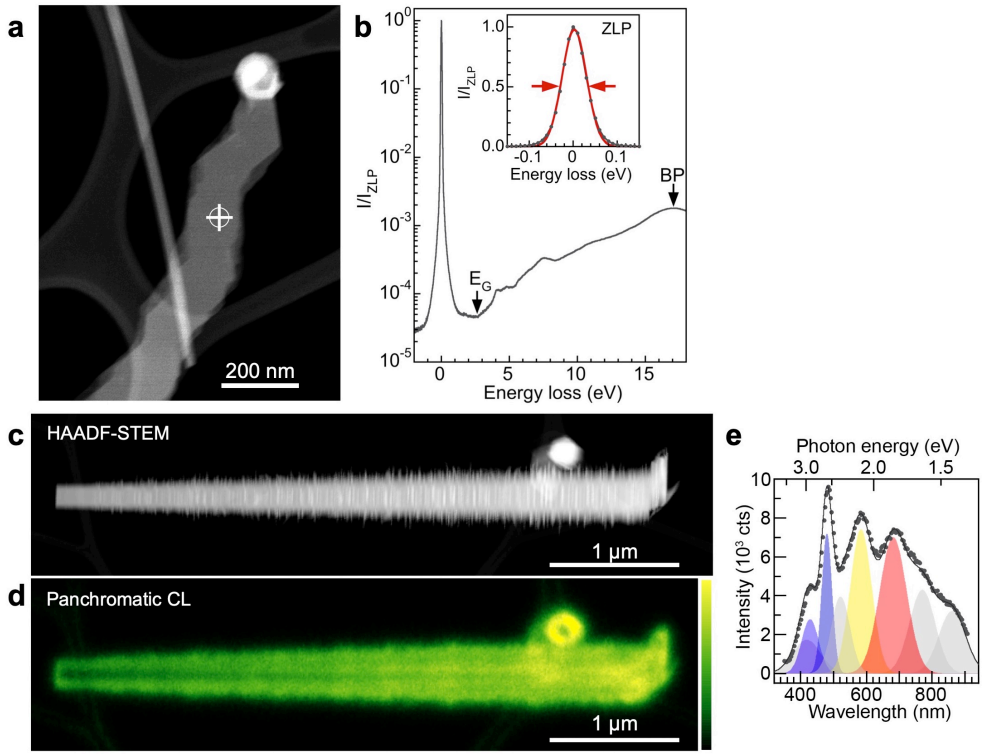

Figure 3. Optoelectronic properties of individual GaS nanowires. a. STEM image of a typical transverse (ribbon-like) GaS wire. Bright contrast at the tip marks the high-Z VLS catalyst particle. **b.** Nanometer-scale optical absorption measurement using monochromated valence EELS (FWHM of the zero-loss peak (ZLP): 65 meV). The loss onset at 2.65 eV corresponds to the fundamental bandgap of the GaS wire. Also visible is the bulk plasmon (BP) at ~17 eV. **c.** HAADF-STEM image of a tapered longitudinal GaS wire with progressively increasing diameter toward the tip (the VLS catalyst broke off during transfer). **b.** Panchromatic CL map (400 nm $\leq \lambda_0 \leq$ 1000 nm) of the wire shown in c. **e.** Local CL spectrum, showing strong blue band-edge emission along with emissions due to transitions between gap states.

Our analysis showed Au catalysts transporting the precursors (Ga_2S, S) equally to the growth front to yield uniform GaS ribbons. Ag catalysts produce tapered longitudinal wires due to a progressively increasing catalyst volume, explained by preferred Ga_2S uptake, decomposition, and retention of Ga in the catalyst.

GaS nanowires are excellent optoelectronic and photonic materials (Figure 3). Nanoscale optical absorption measurements on single GaS ribbons using monochromated EELS showed a wide (2.65 eV) bandgap. STEM-CL detected intense blue luminescence along with longer wavelength emissions from gap states. STEM-CL measurements on single tapered longitudinal nanowires showed interesting photonic properties, notably Fabry-Perot interference of propagating modes confined to the hexagonal cross-section of the wires (Figure 4). The combined results added to our understanding of vdW nanowire growth for a hexagonal

monochalcogenide semiconductor, and they showed properties that are promising for electronics, optoelectronics, and photonics.

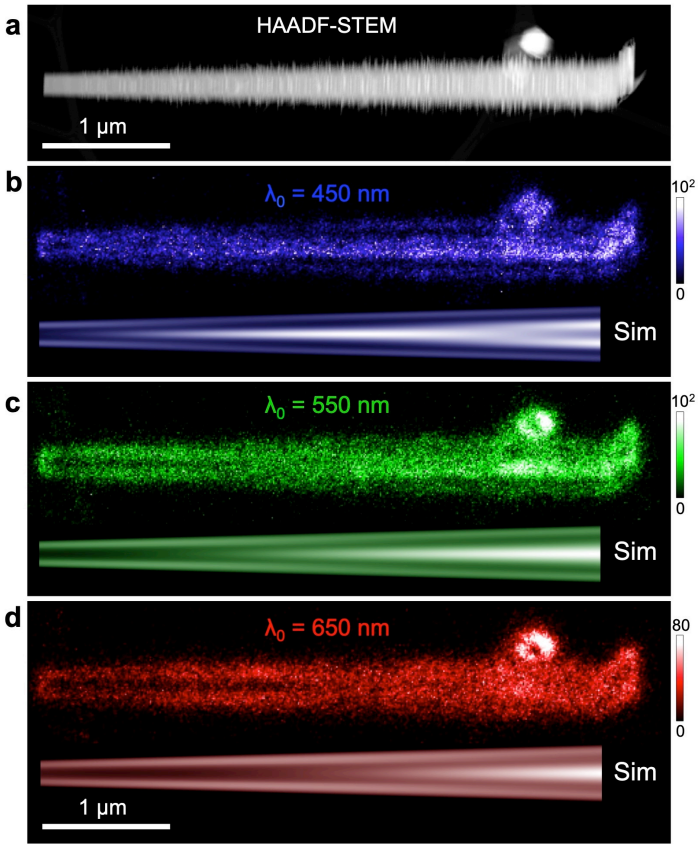

Figure 4. Longitudinal GaS nanowires as Fabry-Perot resonators. a. STEM image of a tapered longitudinal GaS wire. **b. – d.** Monochromatic STEM-CL maps obtained at free-space wavelengths λ_0 of 450 nm (b.), 550 nm (c.), and 650 nm (d.), along with simulations of the intensity distribution due to Fabry-Perot resonances of confined modes propagating across the wire and reflected by its side facets.

2.2. Van der Waals nanowires with continuously variable interlayer twist and twist homojunctions [*Adv. Funct. Mater. 31, 2006412 (2021)*]

Research on GeS nanowires resulted in major advances in our ability to control Eshelby twist *via (i)* homojunctions between twisted and ordinary layered segments, and *(ii)* the realization of continuously varying twist in tapered nanowires.

While most GeS nanowires grow with an axial screw dislocation, we discovered that a sudden temperature drop drives the dislocation from the center to the surface, thus eliminating the defect from the wire (Figure 5). Continued growth produces a defect-free vdW wire attached to the dislocated part, generating a homojunction that seamlessly connects twisted and layered nanowire segments. The formation of such twist homojunctions has immediate implications for the exploration of the effects of helical twist moirés on functional properties, enabling experiments that directly compare the properties of twisted and aligned layered structures in the same nanowire. We performed optoelectronic measurements – nanoscale absorption (EELS) and luminescence (STEM-CL), correlated for the same wires – in the form of linescans across the

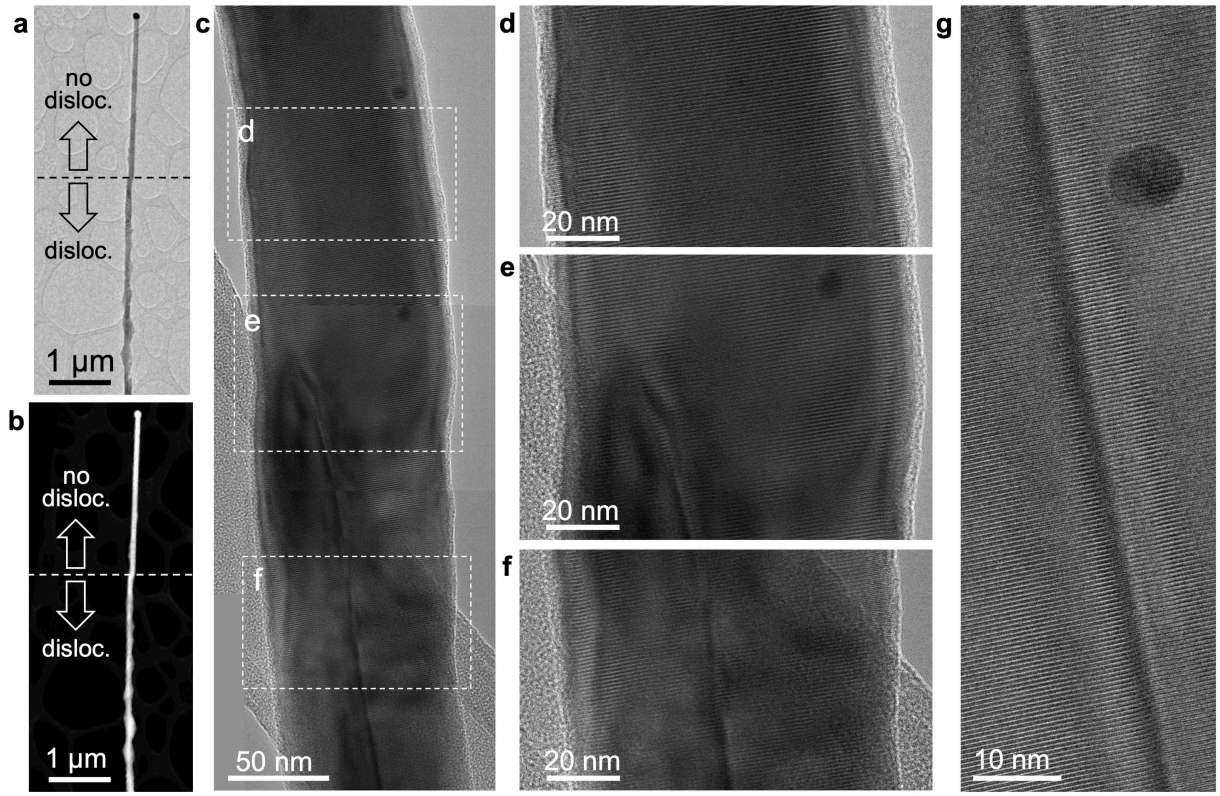

Figure 5. Controlled dislocation ejection during growth creates twist homojunctions in GeS van der Waals nanowires. a. TEM image of the tip portion of a GeS nanowire. The segment between the VLS catalyst at the tip and the horizontal dashed line is defect-free, followed by a long (twisted) segment carrying an axial screw dislocation. **b.** HAADF-STEM image of the nanowire. **c.** High-resolution TEM image near the exit point of the dislocation, whose line bends sharply toward the surface near the center of the field of view. **d. – f.** Magnified views of the regions marked by rectangles in c. **g.** High-resolution TEM image of the screw dislocation.

twist homojunctions (Figure 6). Defect-free portions (no moiré) showed a remarkably constant absorption edge and peak emission energy. In dislocated segments, substantial variations in bandgap and emission energy were observed whose magnitude is consistent with expected bandgap variations between different moiré registries. Positions where the gap is close to that in the non-dislocated wire coincide with regions with the same stacking registry. The ability of creating junctions between defect-free and dislocated segments joined within the same nanowire has provided the basis for demonstrating the striking optoelectronic effects of the interlayer moiré in vdW nanowires.

Other results substantially extended our understanding of Eshelby twist. Experiments on long tapered GeS nanowires for the first time showed a continuous succession of twist angles. This finding implies that each portion of a tapered wire is able to adopt a twist corresponding to its own local diameter with negligible effects by the adjacent wire sections, thus realizing a continuous sequence of interlayer moirés along the helical vdW interface. Our combined results demonstrated unprecedented twist control in vdW nanowires. By connecting twisted and aligned interfaces and integrating a smooth sequence of different moirés, twist junctions and continuously variable twist in helical vdW nanowires define new architectures that have no equivalent in a conventional 2D interface topology.

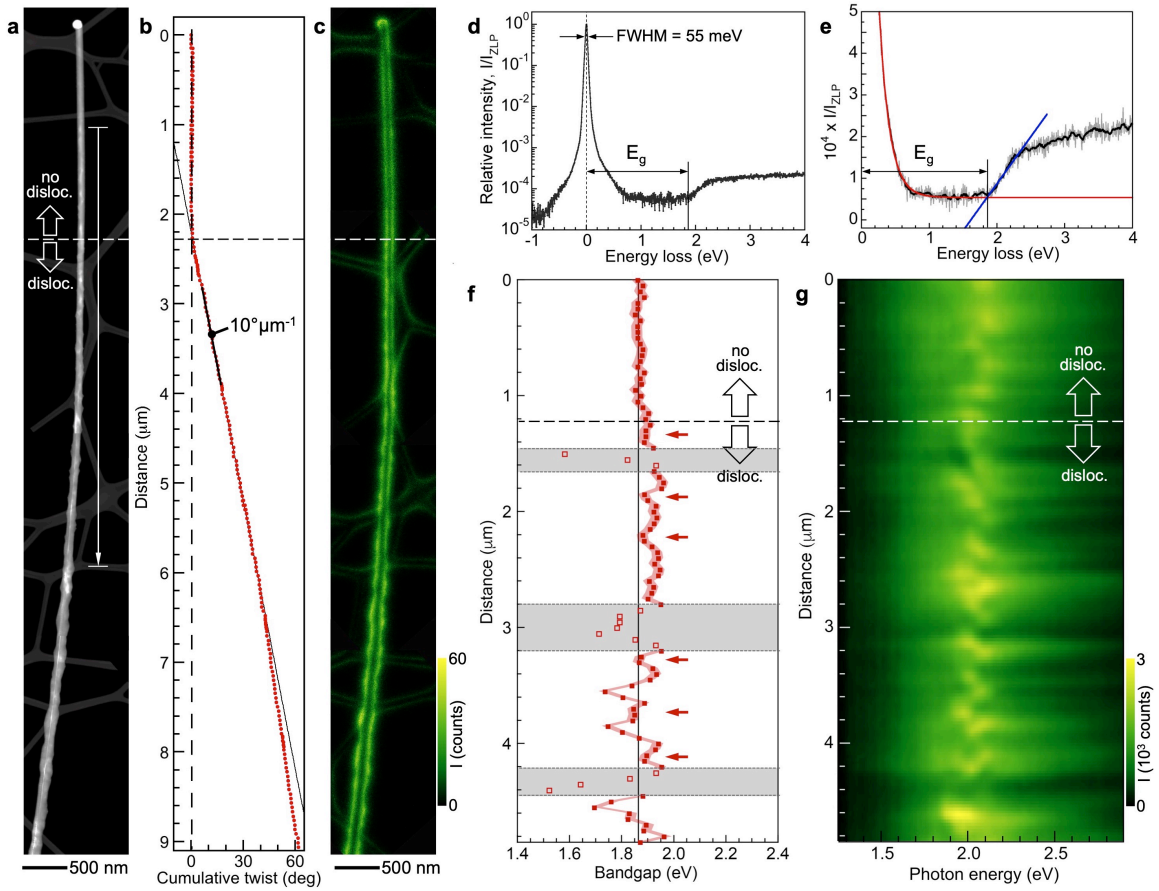

Figure 6. Nano-optoelectronics across twist homojunctions in vdW nanowires. a. HAADF-STEM image of a GeS nanowire comprising joined non-dislocated and dislocated segments. **b.** Nanobeam electron diffraction analysis along the wire shown in a. Note the absence of twist near the tip, and the abrupt onset at the transition to the dislocated wire segment. **c.** Panchromatic STEM-CL map of the nanowire shown in a. **d. – f.** Local absorption measurements by monochromated EELS. **d.** Typical EEL spectrum showing the high energy resolution (FWHM of the zero-loss peak: 55 meV), and the sharp energy loss onset due to GeS interband transitions at the bandgap energy, E_g. **e.** Magnified view of the gap region. Red and blue lines represent fits whose intersection was used to quantify the local absorption edge. **f.** EELS linescan across the twist homojunction (arrow in a.). Note the constant absorption edge (bandgap) in the non-dislocated section and large variations in the twisted segment. Gray bars: Regions of the wire supported by the carbon grid, where no reliable fits of the absorption edge could be obtained. **g.** Hyperspectral STEM-CL linescan along the same portion of the nanowire, coordinated with the EELS linescan shown in f.

2.3. Optoelectronics and nanophotonics of atomically precise GaSe vdW nanoribbons [*Nano Lett. 21, 4335 (2021)*]

Extending our work on Ga chalcogenides from GaS to GaSe, we identified growth processes that lead to free-standing few-layer GaSe nanoribbons with atomically smooth surface and side facets and exceptional optoelectronic/photonic properties. TEM combined with electron diffraction identified them as single crystals with uniform morphology (Figure 7).

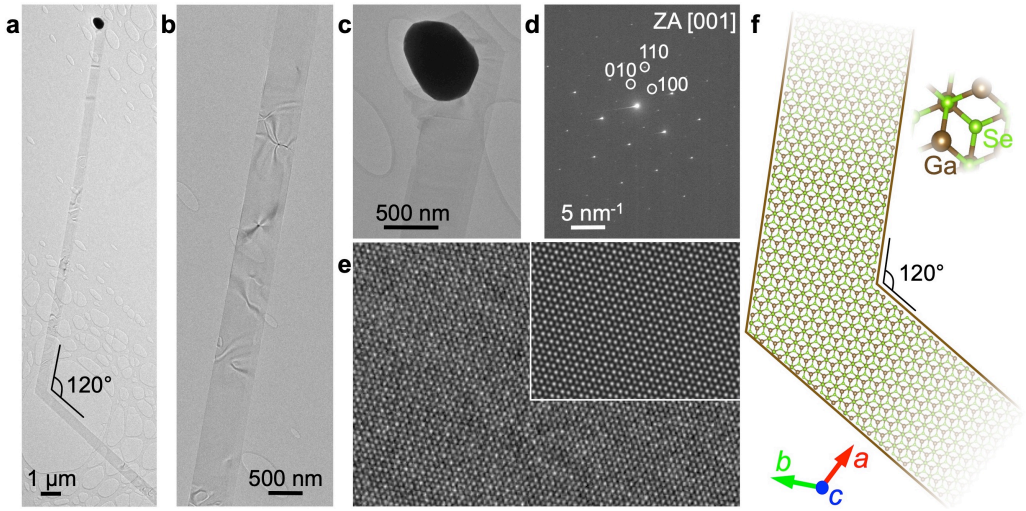

Figure 7. VLS growth of atomically precise few-layer GaSe nanoribbons. a. TEM image of a typical GaSe nanoribbon. Stochastic switching of the catalyst drop produces 120° kinks in a subset of the ribbons. **b.** Higher magnification image of the ribbon shown in a. **c.** Detail of the crystallized VLS catalyst at the tip. **d.** Selected-area electron diffraction demonstrating basal-plane orientation of the ribbon and identifying the edge facets as zigzag edges. **e.** High-resolution TEM image and multislice image simulation (inset) of the ε-GaSe nanoribbon. **f.** Schematic summarizing the structure and morphology of the GaSe nanoribbons.

AFM showed the formation of few-layer GaSe nanoribbons with narrow thickness distribution, atomically smooth surface (RMS height variation of 0.36 nm, *i.e.*, is less than 50% of the thickness of a single GaSe tetralayer (Se-Ga-Ga-Se, ~0.8 nm)), and exceptionally low edge roughness (substantially below 1 nm RMS for a typical ribbon width of 300 – 500 nm).

Optoelectronics and photonics of these few-layer ribbons were investigated by photoluminescence (PL) and cathodoluminescence (STEM-CL). PL on single nanoribbons showed intense, narrow light emission at the GaSe bandgap energy. STEM-CL comparing horizontal and vertical ribbon sections, combined with numerical simulations, yielded unique insight into the nanophotonics of GaSe nanoribbons as well as the excitation mechanisms by an electron beam (Figure 8). CL on horizontal few-layer ribbons, the usual geometry of probing 2D/layered crystals, showed broad, low-intensity spectra without a dominant band-edge component. On the other hand, CL spectra for vertically supported ribbons showed intense, narrow band-edge/excitonic luminescence. These differences could be explained *via* numerical simulations, which established that electron passage next to a horizontal ribbon causes weak and localized induced fields while relativistic electrons passing next to a vertical ribbon coherently stimulate intense propagating waveguide modes. Hence, the intense luminescence observed in CL is due to efficient excitation, propagation of polaritonic modes, and ultimately scattering into free-space photons detected in CL.

The results have implications within the project and more broadly on the ONR "Nanoscale Computing Devices and Systems" program. The findings provide a better understanding of electron stimulated optical excitations in vdW crystals. Specifically, the results demonstrate the excitation of propagating polaritonic modes as an intermediate state between excitation and light emission. Such modes can be a powerful probe of fundamental properties and a potential information carrier, *e.g.*, between qubits. Within the broader programmatic context, our results

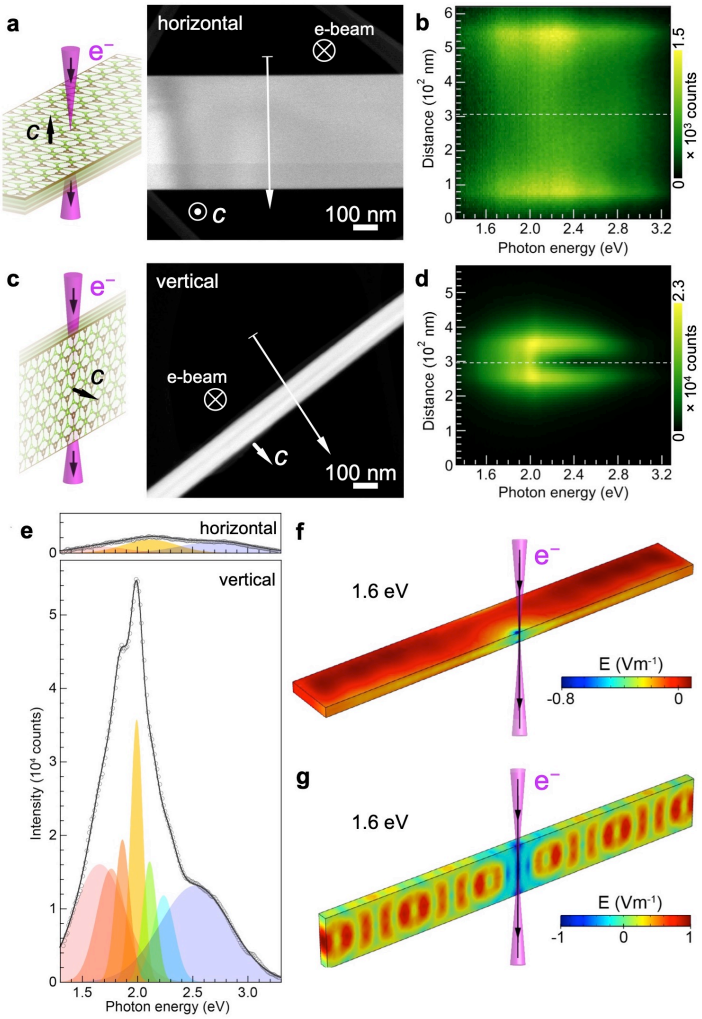

Figure 8. Focused electron beam excitation of GaSe nanoribbon waveguides combined with light detection by CL. a. Schematic of the electron beam excitation of a horizontal GaSe nanoribbon (left) and corresponding STEM image (right). "*c*" denotes the surface normal of the (001) oriented Se-Ga-Ga-Se tetralayers in the GaSe ribbon. **b.** Hyperspectral STEM-CL linescan across the planar ribbon (arrow in a.). **c.** Schematic of the electron beam excitation of a vertical GaSe nanoribbon (left) and corresponding STEM image (right). **d.** Hyperspectral STEM-CL linescan across the standing ribbon (arrow in c.). Note the sharp intensity maximum near 2.0 eV. **e.** Comparison of luminescence spectra obtained in the horizontal and vertical configuration (along the dashed lines in b. and d.), using identical measurement conditions and plotted at the same scale. Electron beam excitation of the horizontal ribbon yields weak, broadband emission while excitation of the vertical ribbon results in a much higher emitted intensity, concentrated in a band-edge/excitonic peak at 2.0 eV. **f. – g.** Numerical simulations of the induced fields resulting from electron beam excitation of a horizontal (f.) and vertical (g.) GaSe nanoribbon. In the horizontal configuration, the induced fields are localized near the beam and weak, while excitation of the vertical ribbon coherently stimulates a propagating polariton wave.

identify chalcogenide analogues to graphene nanoribbons that may be synthesized with comparable fidelity and provide complementary functionality, *e.g.*, as waveguides, single photon sources, *etc*.

2.4. Ultrathin twisted nanowires [*Small 17, 2104784 (2021)*]

In prior work, we obtained twisted GeS vdW nanowires by Au-catalyzed vapor–liquid–solid (VLS) growth with diameters down to ~40 nm, *i.e.*, interlayer twist up to 0.05°. Accessing larger twists requires wires with smaller diameters. Ultrathin wires can also be used to verify the fundamental limits of Eshelby's (elastic continuum) theory for twist in dislocated rods.

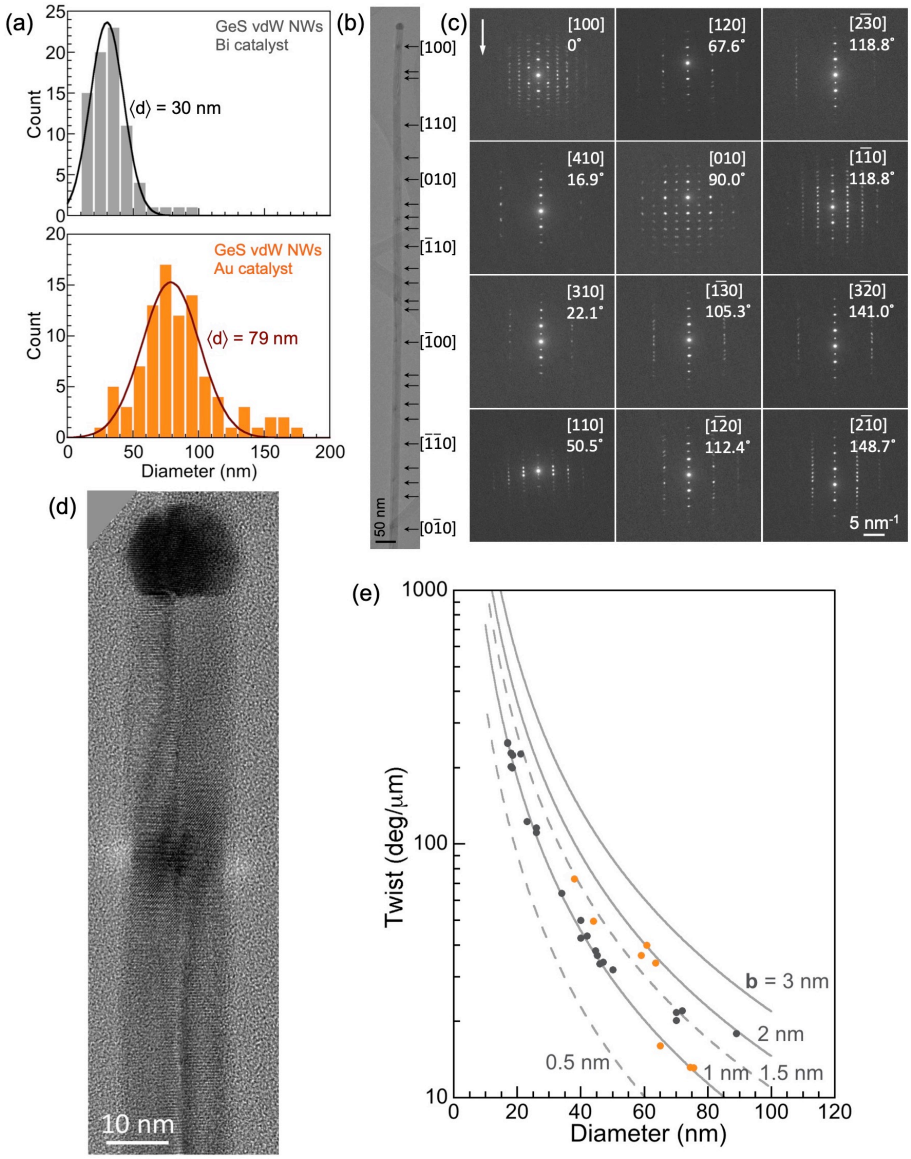

Figure 9. Bismuth catalyzed ultrathin twisted nanowires. a. Comparison of diameter histograms of twisted GeS van der Waals nanowires obtained with Bi and Au catalysts, demonstrating the shift to smaller mean wire diameters achieved in Bi-catalyzed VLS growth. **b.** TEM image of a 15 nm GeS wire with axial screw dislocation, and **c.** associated nanobeam diffraction twist analysis of Eshelby twist. **d.** High-resolution TEM of an ultrathin GeS nanowire, showing the axial screw dislocation in the wire propagating into the Bi particle at the tip. **e.** Verification of Eshelby's theory down to ultrathin dislocated nanowires.

We developed a protocol for the VLS growth of ultrathin dislocated GeS nanowires over Bi catalysts (Figure 9). The use of Bi shifts the mean nanowire diameter to substantially smaller values. We found that even the thinnest (~15 nm) wires consistently carry one axial screw dislocation and closely follow Eshelby's predicted twist. Large interlayer twists in such ultrathin vdW nanowires (up to 0.4°) promise large twist effects, and the small diameters also cause a significant confinement-induced bandgap widening. Finally, we discovered that the dislocation in the nanowires templates a screw dislocation in the Bi tip, which crystallizes epitaxially on the wire at the completion of the growth process (Figure 10). Since Bi is a topological insulator, this controlled introduction of a screw dislocation is expected to yield topologically protected states associated with the dislocation.

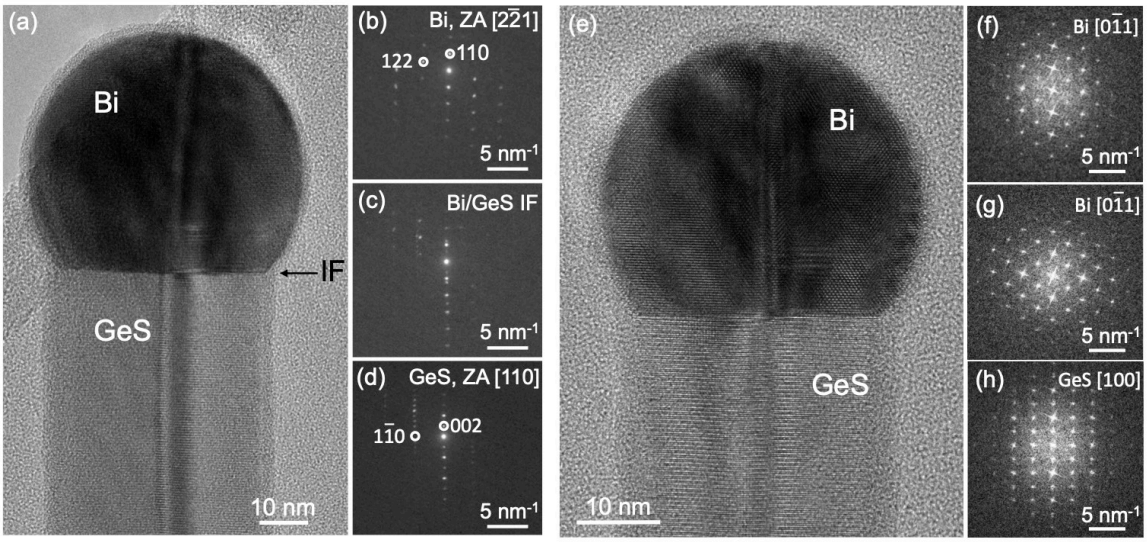

Figure 10. Transfer of screw dislocations from layered GeS nanowires into their Bi tip. a. High-resolution TEM image showing the interface (IF) between a chiral twisted GeS nanowire and its Bi VLS catalyst. Note the continuation of the axial screw dislocation from the nanowire into the Bi crystal. **b. – d.** Diffraction analysis of the epitaxial relationship between Bi and GeS. **e.** High-resolution TEM image showing another example of a Bi screw dislocation templated by the dislocation in the GeS nanowire. **f. – h.** Analysis of the Bi/GeS epitaxial relationship.

2.5. Large, ultrathin ribbons by VLS growth and edge incorporation [*Nanoscale 14, 6195 (2022)*]

Layered GeSe is of interest for its anisotropic properties, direct bandgap, ferroelectricity, and high charge carrier mobility. We demonstrated the VLS growth of large, ultrathin single crystalline GeSe nanoribbons (Figure 11). The characteristic triangular morphology of these vdW ribbons is determined by fast longitudinal VLS growth combined with lateral expansion *via* edge incorporation from the vapor phase. This mechanism produces free-standing ribbons with widths up to 30 μm and lengths exceeding 100 μm while consistently maintaining sub-50 nm thickness. CL spectroscopy on individual GeSe ribbons shows intense band-edge luminescence up to room temperature, in contrast to GeSe flakes obtained by other processes that showed light emission only at cryogenic temperatures, confirming a low concentration of nonradiative recombination centers in the VLS-synthesized GeSe ribbons. Within the broader context of this ONR program, the results identify chalcogenide analogues to graphene nanoribbons that may be synthesized with comparable fidelity and provide complementary functionality, *e.g.*, as waveguides, ferroelectrics, hosts for single photon sources, *etc*.

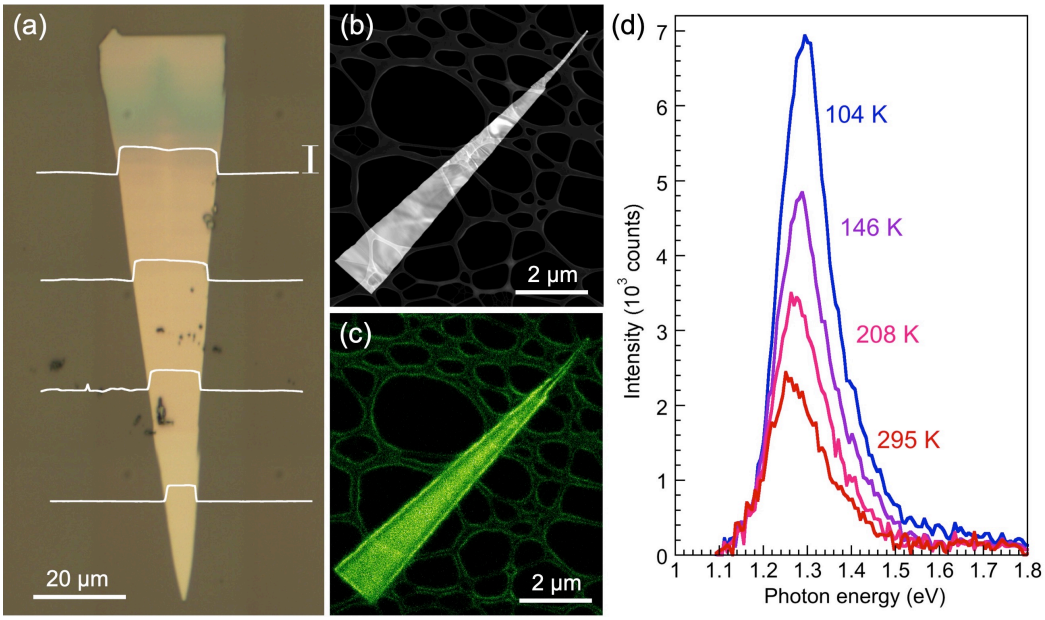

Figure 11. Large, ultrathin GeSe ribbons with low defect density and strong light emission up to room temperature. a. Optical image of a GeSe ribbon with characteristic triangular shape, defined by simultaneous axial VLS growth and lateral expansion by edge incorporation from the vapor. Vertical scale bar: 50 nm. **b.** STEM image, and **c.** panchromatic cathodoluminescence (CL) map of a smaller GeSe ribbon. **d.** CL spectra showing the GeSe band-edge luminescence between 100 K and room temperature.

2.6. Screw-dislocation induced ferroelectricity [*Small 17, 2104784 (2021)*]

Symmetry breaking is a central theme in the quest for new functional materials. Non-centrosymmetric crystals enable a number of functionalities of interest for applications ranging from information processing to energy conversion. Group IV monochalcogenides such as GeS break mirror symmetry only in monolayers and in few-layer crystals with odd layer number. Both have proven challenging to realize experimentally.

We discovered an unusual effect that leads to spontaneous symmetry breaking in monochalcogenide nanowires. Chiral twisted GeS nanowires can host screw dislocations with Burgers vector equal to half the *c*-axis unit cell rather than the usual integer *c*-axis spacing. Crystallographically, this is only possible if the centrosymmetric A-B stacking is replaced by a non-centrosymmetric A-A stacking order. Hence, the introduction of a screw dislocation causes a spontaneous symmetry breaking, which can lead to ferroelectricity in chiral GeS nanowires.

2.7. Orthorhombic germanium diselenide ribbons [*Nano Lett. 22, 7952 (2022)*]

Many materials are known to exist in several stable polymorphs, but synthesis typically provides access only to a subset of these phases. A case in point is the dichalcogenide semiconductor $GeSe_2$. Crystalline $GeSe_2$ invariably adopts the 2D/layered monoclinic β-phase. Hence, the properties of possible other stable polymorphs remain unknown. During our experiments on VLS growth of Ge chalcogenide nanostructures, we discovered an approach for the high-yield synthesis of nanoribbons of the orthorhombic phase of $GeSe_2$ (Figure 12). Access

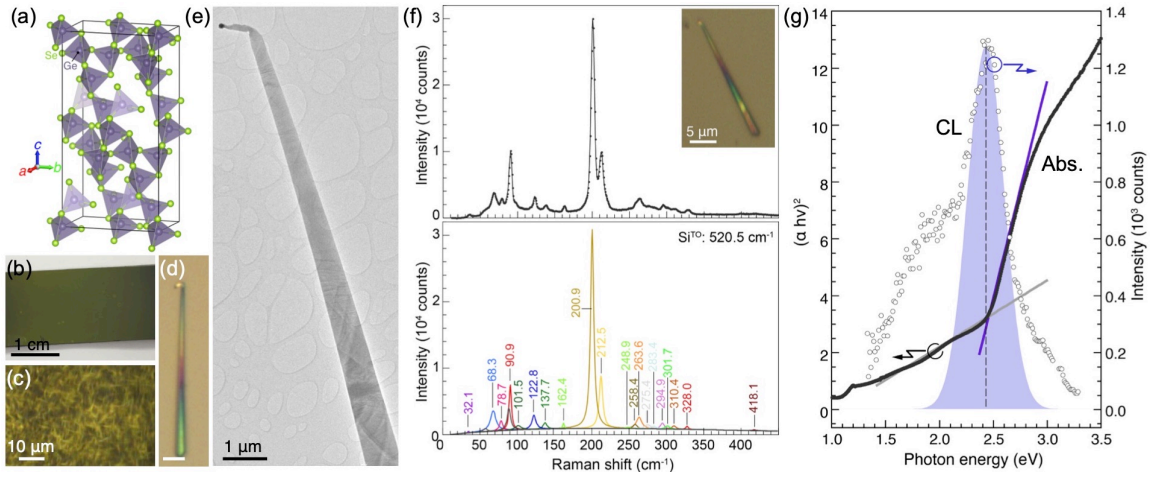

Figure 12. Nanoribbons of a new crystal polymorph – orthorhombic $GeSe_2$: a. Crystal structure of orthorhombic $GeSe_2$. **b. – d.** Optical microscopy: Full sample (b.), micrometer-scale region (c.), and single nanoribbon (d.). **e.** TEM image of a characteristic orthorhombic $GeSe_2$ ribbon. **f.** Vibrational modes of orthorhombic $GeSe_2$. **g.** Optical absorption (ensemble, "Abs.") and luminescence (single nanoribbon, "CL").

to air-stable ribbons enabled investigating the properties of orthorhombic $GeSe_2$, including its vibrational modes, optical absorption, and light emission. Our results established orthorhombic $GeSe_2$ ribbons as a promising wide-bandgap semiconductor nanostructure for applications in optoelectronics and energy conversion.

2.8. Chiral photonics in twisted nanowires [*Mater. Horiz., in press (published online 07/04/2023)]*

We demonstrated chiral optical effects and dislocation-induced electronic modifications that can transform semiconductor nanostructures into multifunctional components for optoelectronics and photonic circuitry. The work overcame two key challenges in the field: *(i)* The controlled synthesis of inorganic nanostructures that are chiral and carry a single electronically active defect, a screw dislocation; and *(ii)* the detection of chirality and dislocation effects in individual nanostructures rather than ensembles. To address the first challenge, we developed a growth process yielding thick, tapered van der Waals semiconductor nanowires that consistently incorporate an axial screw dislocation. Using a suitable thermal protocol during growth, the resulting chiral growth spiral making up a large part of each wire is joined to a non-dislocated (achiral) section, hence enabling the direct comparison of the properties of chiral and achiral segments within the same nanostructure. And whereas conventional chiroptic measurements, such as circular dichroism, can be applied only to larger chiral ensembles, we introduced optical whispering gallery modes as a new probe of chirality and dislocation effects in single nanostructures.

STEM-CL spectroscopy – directly comparing chiral and achiral segments within single GeS nanowires – combined with numerical simulations demonstrated chirality effects in the form of systematic blue shifts of chiral whispering gallery modes (Figure 13). The mode shifts are caused by an altered permittivity tensor of the chiral nanostructures relative to their achiral counterparts. Furthermore, comparison of CL spectra obtained along dislocated and defect-free, thick tapered

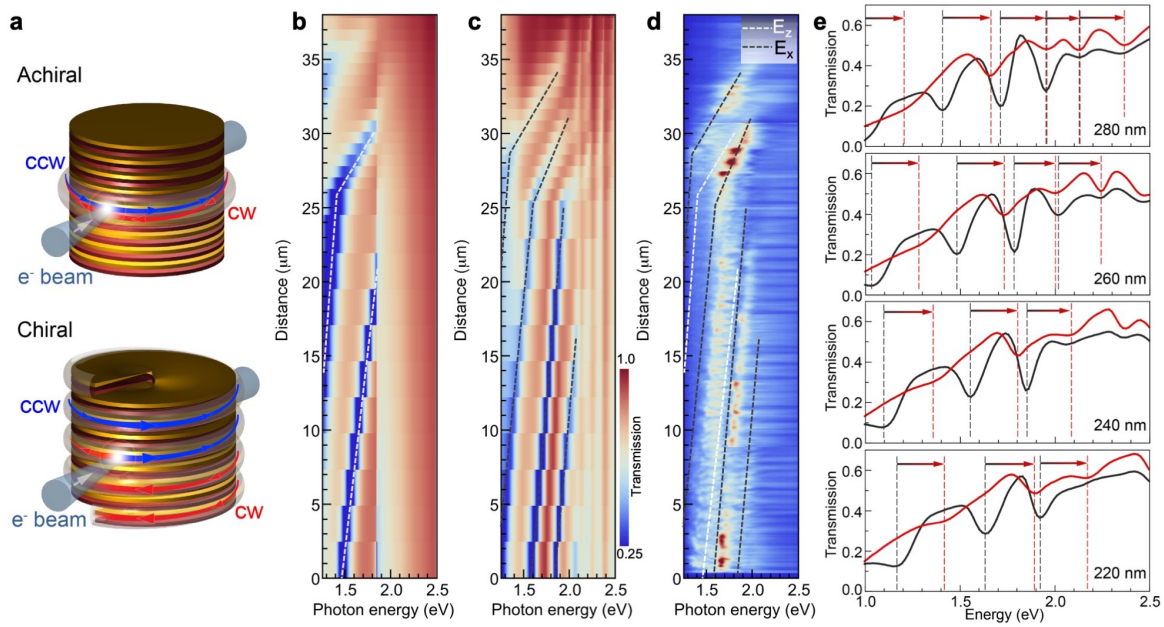

Figure 13. Chiral whispering gallery modes in helical GeS nanowires. a. Achiral and chiral whispering gallery modes in van der Waals nanowires excited by the focused electron beam in STEM. **b.** Simulated transmission of a tangential strip waveguide for E_z excitation of an achiral GeS wire. **c.** Simulated transmission of the strip waveguide for E_x excitation of an achiral GeS wire. Transmission minima in panels b. and c. coincide with energies at which a whispering gallery mode is excited in the adjacent GeS nanowire. **d.** Comparison of the simulations for E_z and E_x excitation with an experimental STEM-CL linescan along a tapered GeS nanowire with joined chiral (0 – 27 μm) and achiral (27 – 38 μm) segments. Note the pronounced blue shift of the measured modes relative to the simulation for E_x excitation in the chiral part of the nanowire. **e.** Numerical simulations demonstrating the blue shift of whispering gallery modes from an achiral (black) to a chiral twisted GeS nanowire (red).

nanowires along the same range of diameters showed a striking modulation of the light emission from wires with axial screw dislocations (Figure 14). Careful analysis ruled out any influence due to a marginally varying registry of the twist moiré pattern in such thick nanowires, and instead pointed to direct dislocation effects on the electronic structure as the cause of the modulated luminescence. The measurements therefore demonstrated whispering gallery modes as a powerful tool for probing the energy landscape along dislocated nanostructures, enabling the detection and investigation of electronic effects of single dislocations.

The combined results opened up a field of research aimed at harnessing nanostructures with inherent chirality and defect-derived functionality for applications such as light emission and detection, sensing, and information processing.

2.9. Transport and chiral magnetoresistance in twisted nanowires [*unpublished results*]

As shown in our research on whispering gallery modes in dislocated nanowires (see above), screw dislocations can strongly affect the electronic structure. Other possible manifestations of direct dislocations effects include the generation of topologically protected states, spin-orbit effects, chiral transport, *etc*. Twisted vdW nanowires are ideal for studying such effects since *(i)* single screw dislocations can be obtained with high fidelity during the synthesis process, and *(ii)*

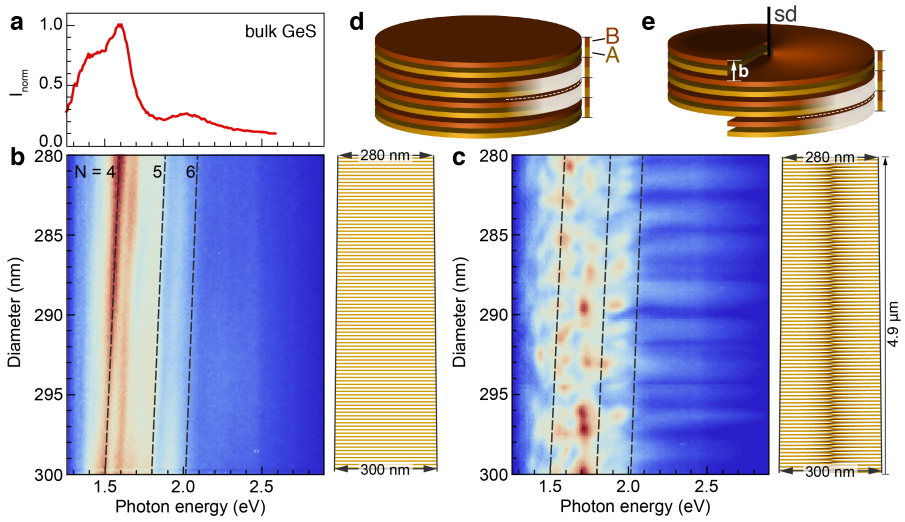

Figure 14. Modulated electronic structure due to single screw dislocations detected by whispering gallery modes in GeS nanowires. a. CL spectrum of a bulk GeS flake, showing the main band-edge peak at ~1.60 eV as well as a characteristic shoulder to lower energies. **b.** Hyperspectral CL linescan along a tapered defect-free GeS nanowire (schematic in d.) covering diameters between 280 – 300 nm. Dashed lines mark the dispersion of whispering gallery modes with index $N = 4$ to 6, calculated using a plane-wave model. **c.** Hyperspectral CL linescan along a segment of a dislocated GeS nanowire (schematic in e.) covering the same range of diameters. Dashed lines are identical to those shown in b. **d.** Layer structure of the defect-free GeS nanowire with equilibrium AB layer stacking. **e.** Dislocated GeS nanowire with Burgers vector **b** of the axial screw dislocation (sd).

large dislocation effects are expected since the screw dislocation lies in close proximity to the entire current-carrying channel.

We performed gated conductance measurements on individual GeS wires with dislocated and non-dislocated segments joined by twist junctions. Measurements at 300 K and zero magnetic field show periodic conductance modulations at positive gate bias, which may be a signature of coherent transport in the twisted wires. Future work will extend these first measurements to low temperature and in in-plane fields to identify the origin of the conductance modulation and detect signatures of chiral magneto-transport.

3. Training Opportunities

The project has provided extensive training opportunities to all participants, which included one postdoctoral associate, several graduate students, as well as two undergraduate students enrolled in the Electrical & Computer Engineering program at the University of Nebraska-Lincoln.

One postdoctoral fellow was provided opportunities for training and career development by carrying out numerical simulations of electron-beam excitations of propagating polariton modes in nanoribbon waveguides and of whispering gallery modes in achiral and chiral GeS nanowires. His contributions resulted in co-authorship of two publications under this project.

The graduate students were provided training relevant to the multifaceted topics of the project, including concepts such as nanowire synthesis, twist effects in 2D/layered crystals, the

chemistry of intercalation into van der Waals crystals, *etc*. The students also received in-depth training in experimental methods, including deposition of metal catalysts for vapor-liquid-solid (VLS) growth, VLS nanowire growth of different van der Waals materials, and characterization by Raman and photoluminescence spectroscopy, atomic force microscopy, optical absorption, *etc*. Finally, the students were also given opportunities for developing experiments and for open-ended investigation. This included, for example, the design of new experimental setups such as an electrochemical cell for liquid-phase intercalation of van der Waals nanowires.

Undergraduate student interns made important contributions to the project throughout its duration. The students were provided with comprehensive training with focus on the synthesis of van der Waals nanowires using metal catalyzed VLS processes. This included the preparation of substrates, deposition of catalyst metals, setup and programming of growth reactors, and synthesis of different van der Waals nanostructures. The students also received training in safe work practices in the laboratory and in the use of characterization methods including optical microscopy, Raman spectroscopy, and photoluminescence. For one of the undergraduates (J.S. French), participation in the project has been particularly stimulating and rewarding, as evidenced by his co-authorship on four peer-reviewed publications from the project.

The project also presented professional development opportunities for to several external collaborators (see "Other Collaborators"), engaging them in research topics outside their core area of expertise.

Finally, the project provided the PIs ample opportunities to further extend their skills in supervision and mentoring. Closely involved in all stages of the project workflow, from experiment design, data acquisition and analysis, to the authoring of publications and presentation of invited and plenary talks, the PIs continued their professional development and acquired new experience and skills.

4. Results Dissemination

From the start of the project in April 2020 to its conclusion in March 2023, results of the ONR funded research have been disseminated in eight peer-reviewed publications, mostly in high-impact journals (see "Products"). Seven of these papers reported original research; the eight was an invited review on "Van der Waals heterostructures" in a Nature family journal (Nature Reviews Methods Primers) authored by a team of international experts in the field under the leadership by the PIs of this project, one of whom served as corresponding author for the article. The tutorial review has been exceptionally well received in the community, as evidenced by over 3700 article accesses and 26 citations in one year since its publication in late July 2022.

The PIs received a substantial number of invitations to deliver plenary, keynote, and invited talks at international conferences, as well as the prestigious "Walter Schottky Seminar" at the Technical University of Munich. Due to the Covid-19 pandemic, most of these meetings were still held virtually/online during large parts of the project. Presentations discussing results from this project and acknowledging ONR support included the following:

1. P. Sutter and E. Sutter, "Riemann surfaces in twisted van der Waals nanowires", ONR Nanoelectronics Program Review, July 9, 2020.
2. E. Sutter, "Combined imaging, nanobeam diffraction, and cathodoluminescence spectroscopy of two-dimensional/layered crystals and nanowires", NIST Virtual Workshop on Current Status and Perspective of In Situ Electron Microscopy for Electronic and Quantum Materials, July 13, 2020. *[Invited]*

3. E. Sutter, “Liquid metal catalyzed 1D semiconductor nanowires, ribbons and heterostructures”, Great Plains Catalysis Society Webinar, November 19, 2020. *[Invited]*
4. P. Sutter, E. Sutter, “Beyond 2D materials: Layered crystals with a twist”, Photonics West Symposium on 2D Photonic Materials and Devices, March 6-12, 2021. *[Invited]*
5. E. Sutter, P. Sutter, “Beyond 2D materials: Layered crystals with a twist”, 2021 American Chemical Society Spring Meeting, Symposium on 2D Materials for Energy, Sensing, and Quantum Information Science, April 12, 2021. *[Invited]*
6. E. Sutter, “Nanoscale optoelectronics of layered crystals, heterostructures and van der Waals nanowires”, 9th International Conference on the Physics of Semiconductors "Jaszowiec", Szczyrk, Poland, June 21-26, 2021. *[Invited]*
7. E. Sutter and P. Sutter, “Chiral twisted van der Waals nanowires”, American Conference on Crystal Growth and Epitaxy (ACCGE-23), August 3, 2021. *[Invited]*
8. P. Sutter and E. Sutter, “Beyond 2D materials: Layered crystals with a twist”, American Conference on Crystal Growth and Epitaxy (ACCGE-23), August 4, 2021. *[Invited]*
9. E. Sutter, “1D nanowires of 2D layered materials: A new frontier in nanomaterials”, 25th Congress and General Assembly of the International Union of Crystallography, Prague, Czech Republic, August 22-29, 2021. *[Invited]*
10. E. Sutter, “New frontiers in two dimensional/layered materials”, International Conference on Functional Nanomaterials and Nanodevices, NanoMat Bratislava, September 6, 2021. [*Keynote*]
11. P. Sutter, “Group IVA chalcogenides – Emerging materials for unconventional van der Waals heterostructures”, 12th International Conference on “Recent Progress in Graphene and Two-dimensional Materials, Yonsei University, Seoul (Korea), October 10-14, 2021. *[Invited]*
12. P. Sutter, “Synthesis of van der Waals materials: Novel heterostructures and control of interlayer twist”, 67th International Symposium of the American Vacuum Society, Virtual, October 25-28, 2021. *[Invited]*
13. P. Sutter, “Teaching layered crystals new tricks: From unconventional heterostructures to twisted nanostructures”, Seminar, Department of Chemistry, Johns Hopkins University, Baltimore (MD), November 9, 2021. *[Invited]*
14. P. Sutter and E. Sutter, “Van der Waals semiconductors: From unconventional heterostructures to twisted nanostructures”, Walter Schottky Seminar, Walter Schottky Institute, Technical University of Munich, January 25, 2022. *[Invited]*
15. P. Sutter, “Unconventional van der Waals heterostructures: Synthesis, nanoscale optoelectronics and photonics”, Photonics West Symposium on 2D Photonic Materials and Devices V, January 26-27, 2022. *[Invited]*
16. E. Sutter, “Nanoscale optoelectronics of layered crystals”, Heterostructures and van der Waals Nanowires, Mechanical Engineering Department, University of Iowa, March 24, 2022. *[Invited]*
17. E. Sutter, “New Frontiers in two-dimensional and layered materials”, International Conference on Functional Nanomaterials and Nanodevices 2022 (NANOMAT2022), Bratislava, Slovakia, September 6, 2022. *[Plenary]*

18. P. Sutter, "Van der Waals nanostructures by vapor-liquid-solid growth", International Conference on Functional Nanomaterials and Nanodevices 2022 (NANOMAT2022), Bratislava, Slovakia, September 6, 2022. *[Invited]*

19. P. Sutter, "Van der Waals semiconductors: From unconventional heterostructures to twisted nanostructures", Colloquium, Department of Physics, University of South Florida, March 10, 2023. *[Invited]*

Results from this project were also disseminated on the research website of the PIs, https://unlcms.unl.edu/engineering/mme/eli-sutter/. Information provided on the site includes research highlights, publications, personnel, *etc*. The website displays the required ONR disclaimer: "Any opinions, findings, and conclusions or recommendations expressed in this material are those of the author(s) and do not necessarily reflect the views of the Office of Naval Research."

5. Participants

- Prof. Peter Sutter, Principal Investigator
- Prof. Eli Sutter, Co-Principal Investigator
- Dr. Larousse Khosravi-Khorashad, Postdoctoral Research Associate
- Ms. Sudha Krishnan, Graduate Research Assistant
- Mr. Sanchaya Pandit, Graduate Research Assistant
- Mr. Jacob Scott French, Undergraduate Student
- Mr. Kyle Lynnell, Undergraduate Student

6. Other Collaborators

- Prof. Christos Argyropoulos, University of Nebraska-Lincoln, Lincoln (Nebraska): Prof. Argyropoulos collaborated with the PIs of this project by carrying out numerical simulations complementing the nano-optoelectronics measurements by STEM-CL.
- Dr. Juan Carlos Idrobo, Oak Ridge National Laboratory, Oak Ridge (Tennessee): Dr. Idrobo collaborated with the PIs of this project by supporting their EELS experiments on the Nion Hermes monochromated and aberration corrected (MAC) STEM as users of the Oak Ridge Center for Nanophase Materials Sciences (CNMS).
- Prof. Cristian Ciobanu, Colorado School of Mines, Golden (Colorado): Prof. Ciobanu collaborated with the PIs by carrying out density-functional theory calculations of the electronic structure of different registries in GeS twist moirés.

7. Products

Peer-reviewed journal publications reporting results from this project and acknowledging ONR support:

1. E. Sutter, J.S. French, S. Sutter, J.C. Idrobo, and P. Sutter, "Vapor–liquid–solid growth and optoelectronics of gallium sulfide van der Waals nanowires", ACS Nano 14, 6117-6126 (2020). DOI: 10.1021/acsnano.0c01919
2. P. Sutter, J.C. Idrobo, and E. Sutter, "Van der Waals nanowires with continuously variable interlayer twist and twist homojunctions", Advanced Functional Materials 31, 2006412 (2021). DOI: 10.1002/adfm.202006412

3. P. Sutter, J.S. French, L. Khosravi Khorashad, C. Argyropoulos, and E. Sutter, “Optoelectronics and Nanophotonics of Vapor–liquid–solid grown GaSe van der Waals nanoribbons”, Nano Letters 21, 4335–4342 (2021). DOI: 10.1021/acs.nanolett.1c00891
4. E. Sutter and P. Sutter, “Ultrathin twisted germanium sulfide van der Waals nanowires by bismuth catalyzed vapor–liquid–solid growth”, Small 17, 2104784 (2021). DOI: 10.1002/smll.202104784
5. E. Sutter, J.S. French, and P. Sutter, “Free-standing large, ultrathin germanium selenide van der Waals ribbons by combined vapor–liquid–solid growth and edge attachment”, Nanoscale 14, 6195-6201 (2022). DOI: 10.1039/D2NR00397J
6. A. Castellanos-Gomez, X. Duan, Z. Fei, H.R. Gutierrez, Y. Huang, X. Huang, J. Quereda, Q. Qian, E. Sutter, and P. Sutter, “Van der Waals heterostructures”, Nature Reviews Methods Primers 2, 58 (2022). DOI: 10.1038/s43586-022-00139-1
7. E. Sutter, J.S. French, and P. Sutter, “Germanium diselenide ribbons with orthorhombic crystal structure”, Nano Letters 22, 7952 (2022). DOI: 10.1021/acs.nanolett.2c02989
8. P. Sutter, L. Khosravi-Khorashad, C.V. Ciobanu, and E. Sutter, “Chirality and dislocation effects in single nanostructures probed by whispering gallery modes”, Materials Horizons, in press (2023). DOI: 10.1039/D3MH00693J

REPORT DOCUMENTATION PAGE

1. REPORT DATE	2. REPORT TYPE	3. DATES COVERED	
		START DATE	END DATE
20230728	Final Performance Report	04/01/2020	03/31/2023

4. TITLE AND SUBTITLE
Riemann Surfaces in Layered Van der Waals Nanowires: Precision Twist Moirés, Nanoscale Solenoids, and Screw Dislocation Spin-Orbit Coupling

5a. CONTRACT NUMBER	5b. GRANT NUMBER	5c. PROGRAM ELEMENT NUMBER
	N00014-20-1-2305	
5d. PROJECT NUMBER	**5e. TASK NUMBER**	**5f. WORK UNIT NUMBER**

6. AUTHOR(S)

Sutter, Peter; Sutter Eli

7. PERFORMING ORGANIZATION NAME(S) AND ADDRESS(ES)	8. PERFORMING ORGANIZATION REPORT NUMBER
Board of Regents of the University of Nebraska-Lincoln University of Nebraska-Lincoln 2200 Vine St Box 830861 Lincoln NE 68503-2427 United States of America	N/A

9. SPONSORING/MONITORING AGENCY NAME(S) AND ADDRESS(ES)	10. SPONSOR/MONITOR'S ACRONYM(S)	11. SPONSOR/MONITOR'S REPORT NUMBER(S)
Office of Naval Research 875 N. Randolph Street, Suite 1425 Arlington, VA 22203-1995		

12. DISTRIBUTION/AVAILABILITY STATEMENT
Approved for public release: Distribution is unlimited

13. SUPPLEMENTARY NOTES

14. ABSTRACT

Twisted van der Waals (vdW) stacks are engineered materials in which a small azimuthal misalignment of the constituent lattices gives rise to an interfacial twist moiré that can support emergent properties such as moiré excitons and correlated electron physics. Conventionally, such twisted structures are realized in a planar geometry by mechanical stacking.

The research reported here pursued a promising alternative architecture for realizing twist moirés: Nanowires synthesized by vapor-liquid-solid growth of layered crystals. vdW nanowires tend strongly toward incorporating axial screw dislocations, and Eshelby twist due to the dislocation stress field spontaneously produces a chiral structure. Such helical nanowires represent a scalable platform for realizing vdW interfaces with small twist angles that are controlled by the wire diameter and stabilized by the screw dislocation. The reported research focused on understanding the synthesis of vdW nanowires, as well as exploring twist effects and related phenomena using leading-edge methods such as electron-beam excited luminescence and absorption spectroscopies, correlated with structural probes on the same vdW nanowires.

By providing a fundamental understanding of twist effects on electronic structure, optoelectronics, and photonics, the project contributed to a scientific basis for technologies critical to the Navy and DOD. Via training and mentoring of the participants, the project also contributed to the education of the military and civilian high-technology workforce.

15. SUBJECT TERMS

Materials science, nanowires, layered crystals, twist moiré pattern, materials synthesis, vapor-liquid-solid growth, optoelectronics, photonics, chirality, chiral photonics, dislocation, germanium sulfide, germanium selenide, germanium diselenide, gallium sulfide, gallium selenide

16. SECURITY CLASSIFICATION OF:			17. LIMITATION OF ABSTRACT	18. NUMBER OF PAGES
a. REPORT	b. ABSTRACT	C. THIS PAGE		
Unclassified	Unclassified	Unclassified	UU	20

19a. NAME OF RESPONSIBLE PERSON	19b. PHONE NUMBER *(Include area code)*
Prof. Peter Sutter, University of Nebraska-Lincoln	(720) 933-4100

INSTRUCTIONS FOR COMPLETING SF 298

1. REPORT DATE.
Full publication date, including day, month, if available. Must cite at least the year and be Year 2000 compliant, e.g. 30-06-1998; xx-06-1998; xx-xx-1998.

2. REPORT TYPE.
State the type of report, such as final, technical, interim, memorandum, master's thesis, progress, quarterly, research, special, group study, etc.

3. DATES COVERED.
Indicate the time during which the work was performed and the report was written.

4. TITLE.
Enter title and subtitle with volume number and part number, if applicable. On classified documents, enter the title classification in parentheses.

5a. CONTRACT NUMBER.
Enter all contract numbers as they appear in the report, e.g. F33615-86-C-5169.

5b. GRANT NUMBER.
Enter all grant numbers as they appear in the report, e.g. AFOSR-82-1234.

5c. PROGRAM ELEMENT NUMBER.
Enter all program element numbers as they appear in the report, e.g. 61101A.

5d. PROJECT NUMBER.
Enter all project numbers as they appear in the report, e.g. 1F665702D1257; ILIR.

5e. TASK NUMBER. Enter all task numbers as they appear in the report, e.g. 05; RF0330201; T4112.

5f. WORK UNIT NUMBER.
Enter all work unit numbers as they appear in the report, e.g. 001; AFAPL30480105.

6. AUTHOR(S). Enter name(s) of person(s) responsible for writing the report, performing the research, or credited with the content of the report. The form of entry is the last name, first name, middle initial, and additional qualifiers separated by commas, e.g. Smith, Richard, J, Jr.

7. PERFORMING ORGANIZATION NAME(S) AND ADDRESS(ES). Self-explanatory.

8. PERFORMING ORGANIZATION REPORT NUMBER.
Enter all unique alphanumeric report numbers assigned by the performing organization, e.g. BRL-1234; AFWL-TR-85-4017-Vol-21-PT-2.

9. SPONSORING/MONITORING AGENCY NAME(S) AND ADDRESS(ES). Enter the name and address of the organization(s) financially responsible for and monitoring the work.

10. SPONSOR/MONITOR'S ACRONYM(S). Enter, if available, e.g. BRL, ARDEC, NADC.

11. SPONSOR/MONITOR'S REPORT NUMBER(S). Enter report number as assigned by the sponsoring/monitoring agency, if available, e.g. BRL-TR-829; -215.

12. DISTRIBUTION/AVAILABILITY STATEMENT. Use agency-mandated availability statements to indicate the public availability or distribution limitations of the report. If additional limitations/ restrictions or special markings are indicated, follow agency authorization procedures, e.g. RD/ FRD, PROPIN, ITAR, etc. Include copyright information.

13. SUPPLEMENTARY NOTES. Enter information not included elsewhere such as: prepared in cooperation with; translation of; report supersedes; old edition number, etc.

14. ABSTRACT. A brief (approximately 200 words) factual summary of the most significant information.

15. SUBJECT TERMS. Key words or phrases identifying major concepts in the report.

16. SECURITY CLASSIFICATION. Enter security classification in accordance with security classification regulations, e.g. U, C, S, etc. If this form contains classified information, stamp classification level on the top and bottom of this page.

17. LIMITATION OF ABSTRACT. This block must be completed to assign a distribution limitation to the abstract. Enter UU (Unclassified Unlimited) or SAR (Same as Report). An entry in this block is necessary if the abstract is to be limited.